— *PCCP* —

On the Intersystem Crossing Rate in a Platinum(II) Donor-Bridge-Acceptor Triad

G. A. Farrow,[a] M. Quick,[b] S. A. Kovalenko,[b] G. Wu,[a] , A. Sadler,[a] D. Chekulaev,[a] A. Chauvet,[a] J. A. Weinstein,[a]* and N. P. Ernsting[b]*

[a] *Department of Chemistry, University of Sheffield, Sheffield, S3 7HF, UK.*

[b] *Department of Chemistry, Humboldt-Universität zu Berlin, Brook-Taylor-Str. 2, 12489 Berlin, Germany*

Supporting Information

1. The acceptor-only precursor NAP-Pt-Cl [**3**] (*cf.* Scheme 1)

In the main text we concentrated on the photochemistry of the donor-bridge-acceptor triad NAP-Pt-PTZ [**1**]. Spectra were flanked by those of the chemical precursor, NAP-Pt-Cl [**3**], mainly to demonstrate the effect of introducing the acceptor moiety PTZ. But here in the Support, in this section, we discuss our results for NAP-Pt-Cl in their own right.

Transient absorption spectra of NAP-Pt-Cl have already been reported in the visible range.[1] For the current work we extended the spectral coverage in the UV, improved the time resolution, and increased the signal/noise ratio. Dichloromethane (dcm) was used as solvent throughout, in a flow cell with 0.5 mm internal path length and fused-silica windows 0.2 mm thick. The excitation wavelength was centered at 405 nm. The spectral evolution was already shown in **Fig. 1a** of the main text. From multiexponential analysis one obtains the essential TA result, the decay-associated spectra (DAS) which were shown in **Fig. 2a**. The exponential term with decay time $\tau_d=\infty$ (constant contribution – black line in the figure) has a spectrum which shows the bleached ground-state absorption around 23700 cm^{-1} and a broad product absorption band peaking at 15800 cm^{-1}. The latter is attributed to the ^{3}NAP state in agreement with previous studies. An exponential term with decay time τ_c = 193 ps dominates the temporal evolution. Its spectrum (red line) exhibits the band for stimulated emission, having ΔOD < 0 around 19100 cm^{-1}. Decay time τ_a = 0.97 ps has dispersive spectral shape (blue line). We see later that it accounts for a fast red-shift of the stimulated emission band. A smaller, slower red-shift is indicated by the dispersive shape for τ_b = 59 ps (gray line). Lastly note that the induced absorbance at and around the pump wavelength stays constant throughout, meaning that ground-state recovery on this time-scale is not observed with [**3**].

Quantitative connection to the stationary optical spectra is made in **Fig. S1**. Here we focus on the final slow (193 ps) process which is denoted K $\rightarrow$ L. The species-associated spectra (SAS) of the precursor state K and the product state L are shown as red and black lines

(DAS_c+DAS_d and DAS_d, respectively). The stationary absorption spectrum is shown as bleach $-\alpha(\tilde{\nu})$ (dashed black line at right). The spectrum for stationary *stimulated emission* or *gain* $-\gamma(\tilde{\nu}) \sim F(\tilde{\nu})/\tilde{\nu}^2$ (dashed black line at left) was obtained from the spontaneous fluorescence spectrum, *i.e.* the distribution $F(\tilde{\nu}) = \partial\Phi/\partial\tilde{\nu}$ of photons over wavenumbers. The amplitudes of the stationary bands, with which they appear in the transient spectra, are discussed next.

The ground-state absorption band $\alpha(\tilde{\nu})$ is considered first. Fortuitously, a narrow absorption feature exists at 28750 cm^{-1}. It is also observed - as bleach - in the SAS of product state L. By adding an appropriately scaled absorption band, the bleach is compensated for *in silico* and one obtains the excited-state absorption (ESA) spectrum of L. The scale factor is found by the condition that the latter should no longer exhibit structure around 28750 cm^{-1}. In this way the thin gray line in **Fig. S1**, and hence the amplitude of $\alpha(\tilde{\nu})$ in the transient spectra is found. Using that scale factor, we also obtain the ESA spectrum of the precursor state L.

The gain band $\gamma(\tilde{\nu})$ is only partly seen in the SAS of precursor state K, namely as a region in the red spectral region where the induced optical density ΔOD < 0. Note that the band integrals $\int \alpha/\tilde{\nu}\, d\tilde{\nu}$ and $\int \gamma/\tilde{\nu}\, d\tilde{\nu}$ are proportional to the respective electronic transition dipole moment squared, $|M_{up}|^2$ and $|M_{down}|^2$. For the figure we assume that their ratio is 1:0.80, as when the electronic transition in emission is similar (but slightly weaker) to that in absorption. Playing with the ratio we find that the downward "bulges" in the SAS of the emitting state K can be described by bleach and gain bands only if they have amplitude ratios between 1:1 and 1:0.80. Only within this bracket are excited-state absorption spectra predicted to be positive and well-behaved. *The ESA peak at 15350 cm^{-1} may correspond to a ground-state UV absorption at 260 nm*.

We conclude that the emitting state, the one that has 193 ps lifetime after faster spectral relaxations have subsided, has dipole moment squared $|M_{down}|^2$ for radiative transition to the electronic ground state which is of the same magnitude as that for optical absorption.

Broadband fluorescence upconversion (FLUP) spectroscopy[2] provides a complementary view of the excited-state dynamics of NAP-Pt-Cl. The spectral evolution was shown in **Fig. 3a,c.** In general, fluorescence spectra are formatted for stimulated emission as described in the main text. From multiexponential analysis one obtains the essential FLUP result, the decay-associated spectra which were shown in **Fig. 4a**. The main contribution (green line) has τ_c = 193 ps, and its shape matches the stationary emission spectrum (dashed black line). Time constant and shape are practically identical (within experimental error) to those of the transient absorption band for stimulated emission (*cf.* **Fig. 2a** for $\tilde{\nu}$ ≤ 23000 cm^{-1}). For example, a contribution with 1.21 ps corresponds to the fast red-shift which was already seen by TA. Overall, the ~1 ps and 193 ps dynamics observed by transient absorption, are explained quantitatively by shift and decay of stimulated emission.

Femtosecond stimulated Raman (FSR) spectroscopy has been developed for over a decade.[3] We used ps Raman pump pulses at 683 nm, corresponding to 14640 cm^{-1} at the left border of **Fig. 1**. No Raman signal is expected from the electronic ground state due to lack of resonance with the stationary absorption band. At late time, say at 1 ns, the only electronic resonance comes from the broad electronic band peaking at 16000 cm^{-1} with some vibrational structure. The underlying species has already been assigned to ^{3}NAP. The DAS for τ_a = 0.97, τ_b =59, τ_c =193 ps (blue, grey, red lines in **Fig. 2a**) all have effectively decayed to zero and therefore play no role in the stimulated Raman process then. Raman probing was performed at the Stokes side, covering 50-1800 cm^{-1}. Actinic pump pulses at 388 nm (25770 cm^{-1}) were used, and effects due to rotational diffusion were eliminated by appropriate "magic" polarisation angles. Thus, we are set up to interrogate the rising ^{3}NAP population with resonance Raman spectroscopy.

FSR spectra for NAP-Pt-Cl were shown in **Fig. 5**. The delay range t= -150 ps to 1300 ps was recorded in 3 ps steps for the actinic pump pulses, relative to Raman pump/probe pulses at t=0. In the figure we show the evolution for delay times 3-450 ps. Negative-going lines represent Raman gain due to intermediates or products of the photochemical reaction(s). Positive-going lines, at 284 and 702 cm^{-1}, are caused by dichloromethane molecules in the solvent shell.[4] The apparatus function (fwhm = 0.47 ps) was found by examining the rise behavior of the solvent lines with separate measurements (20 fs steps).

Global analysis shows single exponential decay (time constant 197 ps) and a constant term. The characteristic changes are cast into a precursor-successor scheme K $\rightarrow$ L; the species-associated spectra are shown in **Fig. S2**. The process is accompanied by significant change of vibrational line positions. For example a vibrational line at 1195 cm^{-1} appears initially, i.e. in state K. While the amplitude of this line decays, a neighboring line at 1225 cm^{-1} rises with the same 197 ps kinetics ("red" to "black" conversion in the upper panel of **Fig. S2**). In the low-frequency window the most prominent feature is an initial K-mode at 149 cm^{-1}. It decays (again with 197 ps) but without corresponding growth in the neighborhood. This mode was already observed in the time domain (**Fig. 2c**). Clearly the product L is identical with ^{3}NAP, and its precursor K on a 200 ps time scale must be the excited electronic state S that, by fluorescence, was found to have 193 ps lifetime.

2. Experimental details regarding femtosecond stimulated Raman spectroscopy of NAP-Pt-Cl and NAP-Pt-PTZ

Sample solutions were flown through a cell having about 0.5 mm internal path length, as before. Concentrations were adjusted to ~3 OD at the wavelength of the actinic pump (388 nm). Absorption spectra of the sample solutions were measured before and after measurements, and no deterioration was observed. For details of the experimental setup the reader is referred to ref.5.[5]

Time-ranges and -steps were different for the two compounds. NAP-Pt-Cl was measured from -150 ps to +1300 ps in 3 ps steps. For temporal analysis the data were restricted to delay times 3 ps ≤ t ≤ 450 ps and Stokes wavenumbers 50 ≤ $\tilde{\nu}$ ≤ 1800 cm^{-1}. NAP-Pt-PTZ was measured from -2 ps to +8 ps in 20 fs steps and then to 81 ps in 200 fs steps. For analysis

the transient spectra were restricted to $1000 \leq \tilde{\nu} \leq 1600$ cm^{-1}. (Extending the lower limit to 50 cm^{-1} did not show low-frequency lines of significance.)

Broad electronic background had to be removed prior to showing transient Raman spectra. In a first step, a representative spectrum averaged over negative delay times was subtracted. In a second step, all lines other than the two solvent lines were considered to be negative. With this assumption the remaining electronic background could be identified and was removed.

Diminishing spatial overlap of the three beams in the sample cell is responsible for a linear decrease, on a ns time scale, of the amplitude of the solvent lines. To correct for this effect, all FSR spectra have been normalized to the peak of the 702 cm^{-1} solvent line. Furthermore, the data matrix signal($\tilde{\nu}$,t) is cleaned of some noise in a model-free manner using Singular Value Decomposition (SVD). It is from this de-noised matrix that the spectra shown were taken. From experience we may trust vibrational lines that have $|\Delta OD| \geq 10^{-4}$.
A comment is in order on the 149 cm^{-1} Raman line which belongs to the S* state of NAP-Pt-Cl (**Fig. 5b**). An equivalent line was not observed by us with NAP-Pt-PTZ, probably because the signal level was not sufficient. This does not mean that the line in question does not exist; our results are inconclusive in this regard.

The resolution of fast processes is different in the two cases. Because of coarse (3 ps) stepping over NAP-Pt-Cl, the temporal analysis started at 3 ps, and processes with time constants < 10 ps cannot be observed in principle. With NAP-Pt-PTZ stepwidths were 20 fs at first, and the analysis (from – 2 ps) covered the time window of the actinic excitation pulse around time-zero.

Data treatment and analysis was done on the *Wolfram Mathematica* platform. Programs were written specifically for the four types of observations and results. For compound [**1**], time constants of global fits to FLUP and FSR data had the following 68% confidence intervals:

FLUP of [**1**]: τ_a=0.61±0.25 ps, τ_b = 1.65±0.40 ps, τ_c =9.53 ±3.0 ps, τ_d =53.6±20 ps.
FSR of [**1**]: τ_a = 1.60±0.41 ps, τ_b = 5.90±0.90 ps, τ_c =18.2 ±2.9 ps.

Figures

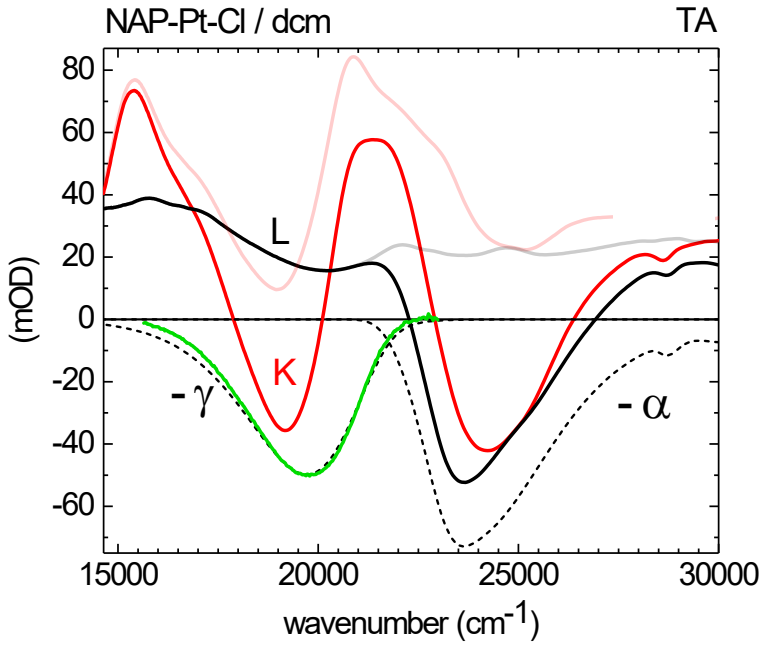

Fig. S1 Species-Associated Spectra (SAS) for transient absorption (TA) of NAP-Pt-Cl, for the final slow (193 ps) process denoted K → L. They are compared to stationary-state spectra for bleached absorption (-α) and stimulated emission or gain (-γ). The amplitudes for α, γ are chosen such that their band integrals have ratio 1:0.80. The predicted excited-state absorption spectra, for these amplitudes, of the transient states K and L are shown as light-red and gray lines, respectively. The green line shows the main upconversion DAS of **Fig. 4** (193 ps component).

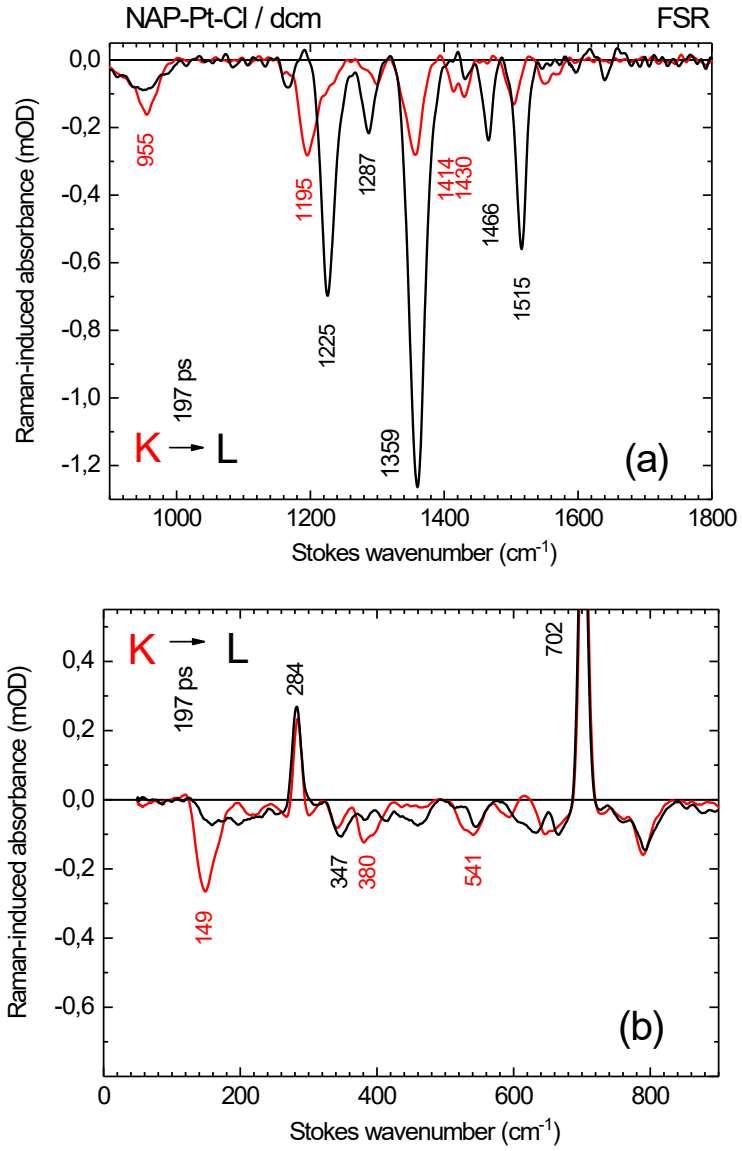

Fig. S2 Species-associated spectra (SAS) for the FSR data in **Fig. 5a,b**, assuming a state sequence $K \rightarrow L$

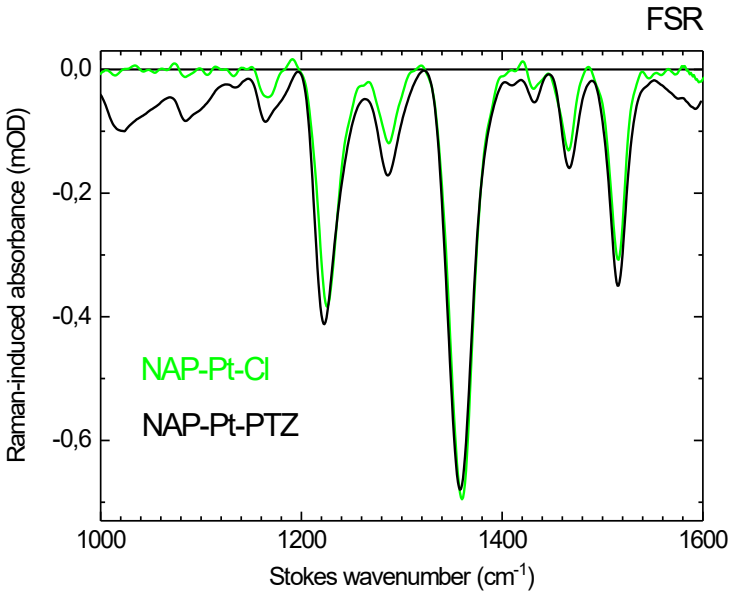

Fig. S3 The resonance Raman spectra of the product states of NAP-Pt-PTZ and NAP-Pt-Cl are practically identical (black and green lines, respectively). This proves that the ^{3}NAP state is formed by both compounds.

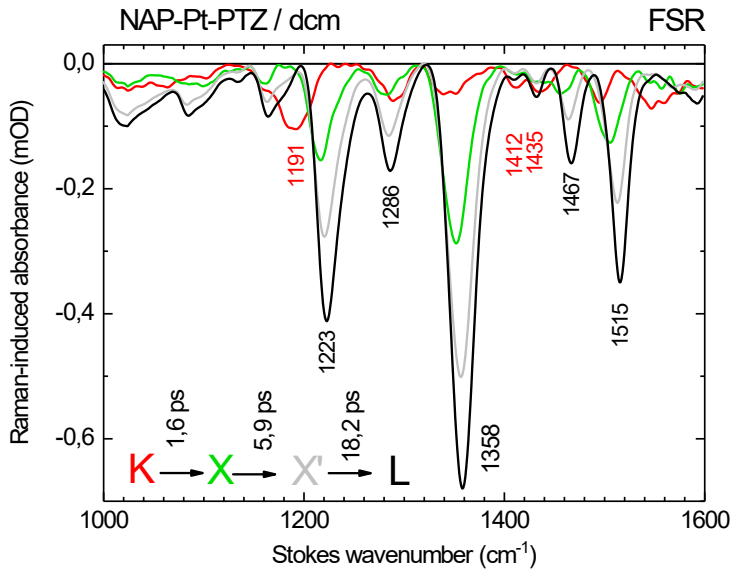

Fig. S4 Species-associated spectra (SAS) for the Raman data in **Fig. 6**, assuming a virtual state sequence K → X→X' →L for simplicity and visualization. Vibrational lines change during the initial (1.6 ps) process K→X. Thereafter the lines observed in state X only grow, in a biexponential fashion, to reach stationarity in product state L.

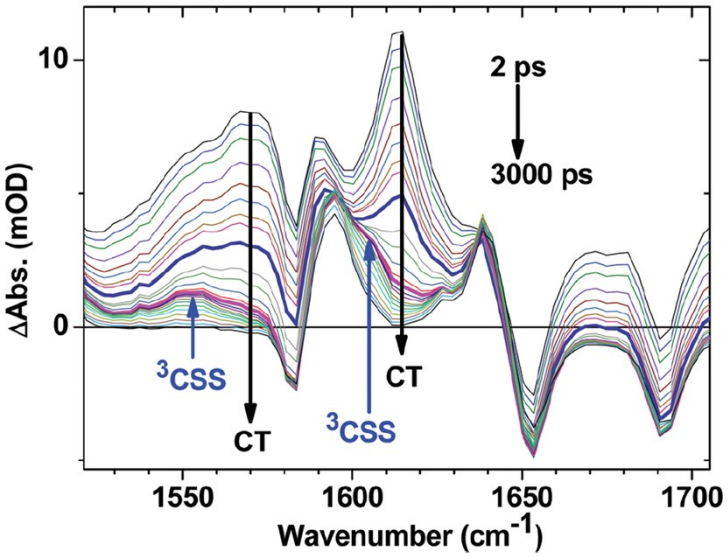

Fig. S5 Reproduction from Ref. 42, of Fig. 6 there showing the extended fingerprint region of the TIR data for [**1**].

Infrared lines at 1590 cm^{-1} and 1640 cm^{-1} are observed after 1 ns and therefore belong to the local triplet state ^{3}NAP. When the earlier history of those lines was examined, it was concluded that they exist already close to time zero, embedded in a broad background due to the charge-transfer character of the excited manifold. As the strong and sloping background falls away in picoseconds, the IR absorbance at the positions of the two lines remain constant, and the lines emerge. This transient infrared result was taken to indicate that ^{3}NAP is created ultrafast. The electronic behavior (for example, quantitative comparison of optical bleach- and gain band amplitudes over time) was left for further clarification.

Instead we consider the possibility that the noted infrared lines of educt and product states may be very similar. In that case precursor-successor kinetics would go undetected by transient IR spectroscopy, and a different experiment must be used, for example femtosecond stimulated Raman (FSR) scattering as in the current paper.

Returning to the previous TIR data, as shown above, we demonstrate in the main text that they are consistent with the model proposed in **Fig. 7**. Finally note that bleached lines are still present in the TIR spectra reproduced above, whereas the (effectively) constant bleach (determined from the red line in **Fig. S7** below) has been removed throughout in the current revision.

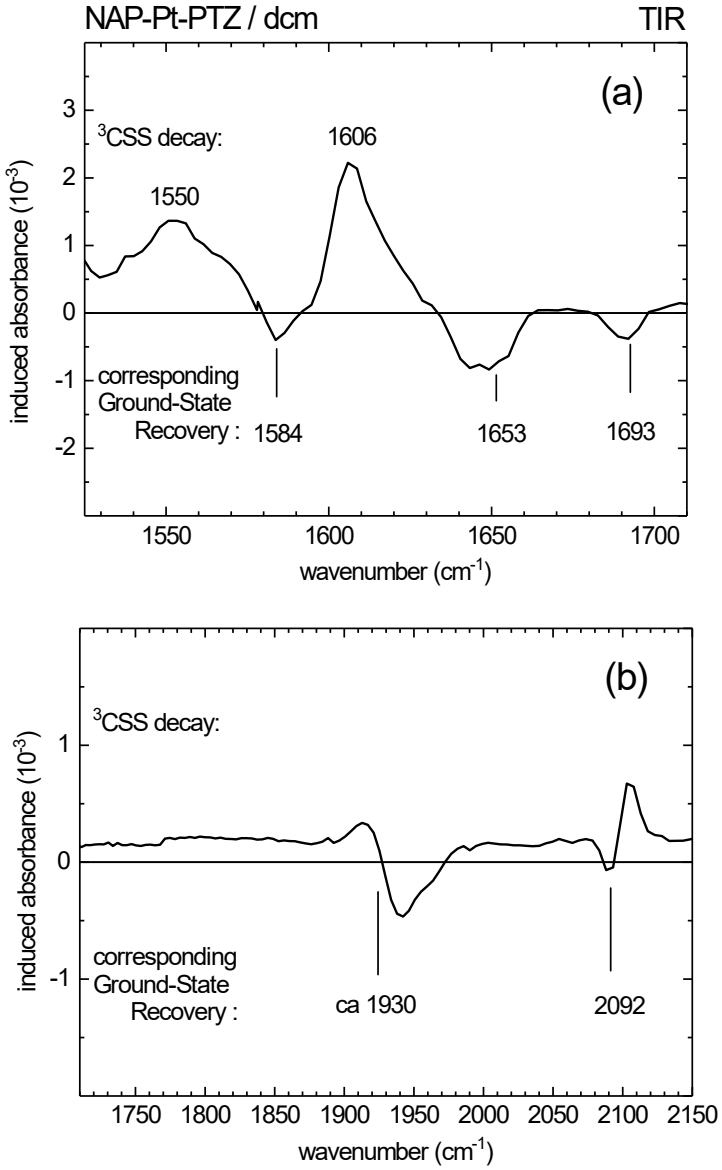

Fig. S6 Transient-infrared DAS for the ~1 ns component, showing the difference IR spectrum of ^{3}CSS.

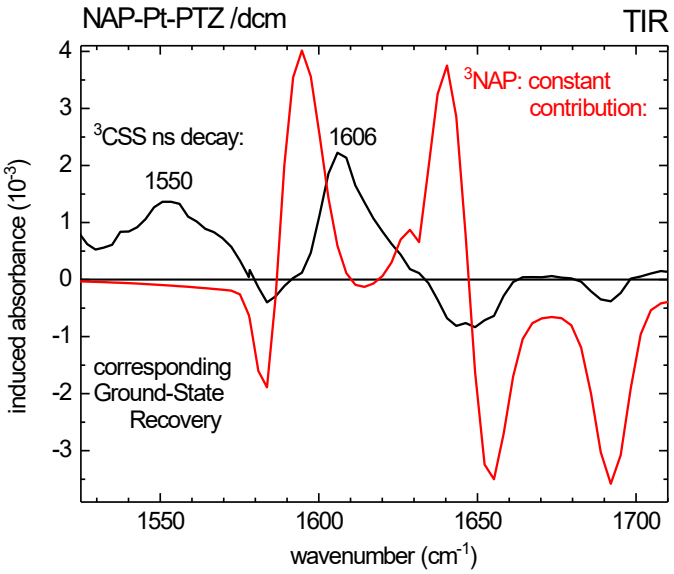

Fig. S7 Transient infrared Decay-Associated Spectrum for the ~1 ns component (black line) from **Fig. S6a**, compared to the constant contribution (red line) which remains at long times (μs). The latter consists of ^{3}NAP product bands (>0) and the bleached S_0 spectrum (bands and some background <0). From the areas under the narrow bleached band at 1693 cm^{-1}, we estimate the relative yields ^{3}CSS:^{3}NAP ≈ 15:85.

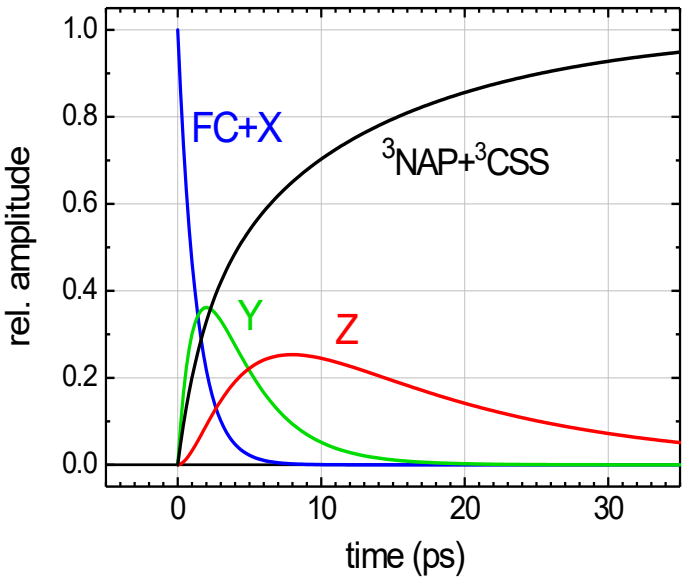

Fig. S8 Amplitude time traces of the SAS in **Fig. 10**.

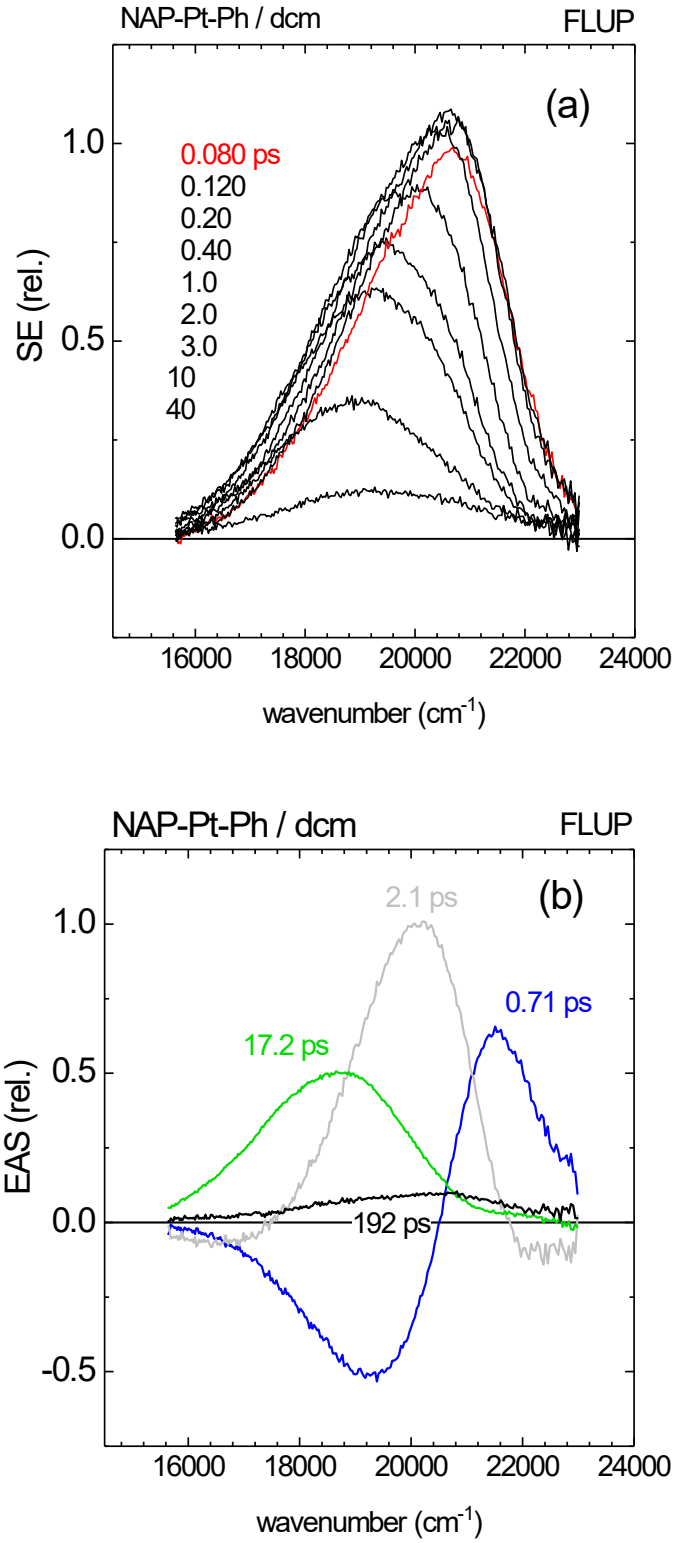

Fig. S9 (**a**) Fluorescence upconversion (FLUP) spectra for NAP-Pt-Ph in dcm, as in **Fig. 3.** (**b**) Decay-Associated Spectra (DAS) for NAP-Pt-Ph, from a global analysis of the transient emission spectra in the panel above. Remember that the effect of finite pulse duration has been deconvoluted from the DAS spectra.

References

1 P. A. Scattergood, M. Delor, I. v. Sazanovich, O. v. Bouganov, S. A. Tikhomirov, A. S. Stasheuski, A. W. Parker, G. M. Greetham, M. Towrie, E. S. Davies, A. J. H. M. Meijer and J. A. Weinstein, *Dalton Transactions*, 2014, **43**, 17677–17693.

2 M. Gerecke, G. Bierhance, M. Gutmann, N. P. Ernsting and A. Rosspeintner, *Rev. Sci. Inst.*, 2016, **87**, 053115.

3 D. R. Dietze and R. A. Mathies, *ChemPhysChem*, 2016, 17, 1224–1251.

4 M. Quick, M. A. Kasper, C. Richter, R. Mahrwald, A. L. Dobryakov, S. A. Kovalenko and N. P. Ernsting, *ChemPhysChem*, 2015, **16**, 3824–3835.

5 S. A. Kovalenko, A. L. Dobryakov and N. P. Ernsting, *Rev. Sci. Inst.*, 2011, **82**, 063102.